Eur. Phys. J. Appl. Phys. **50**, 20401 (2010)
DOI: 10.1051/epjap/2010033

THE EUROPEAN PHYSICAL JOURNAL APPLIED PHYSICS

Regular Article

Characterization of a newly synthesized organic nonlinear optical crystal: benzoyl valine

T.K. Kumar[1], R.S. Selvaraj[1], S. Janarthanan[1], Y.C. Rajan[2], S. Selvakumar[3], S. Pandi[1], M.S. Selvakumar[4], and D.P. Anand[5,a]

[1] Department of Physics, Presidency College, Chennai-600005, India
[2] Department of Materials Science & Engineering, National Chiao Tung University, Hsinchu-300, Taiwan
[3] Department of Physics, L.N Government College, Ponneri-601204, India
[4] Department of Chemistry, St. Xavier's College, Palayamkottai-627002, India
[5] Department of Physics, St. Xavier's College, Palayamkottai-627002, India

Received: 15 September 2008 / Received in final form: 1st September 2009 / Accepted: 1st February 2010
Published online: 26 March 2010 –

Abstract. Herein the synthesis and the crystal growth of benzoyl valine (BV), an organic nonlinear optical (NLO) material for frequency conversion was grown by slow evaporation solution growth technique at room temperature has been reported. The compound was prepared by Stockman method of benzoylation. The solubility curve shows linear nature up to a temperature of 313 K. XRD study reveals that the crystal belongs to monoclinic system with $P2_1$ non-centrosymmetric space group. The fundamental vibrational frequency of various functional groups (400−4000 cm^{-1}) in the crystal was determined from FTIR analysis. ^1H and ^{13}C NMR spectral studies reveal the presence of proton and carbon network in the grown crystalline sample. The optical behaviour of the crystal was ascertained by optical UV absorption spectral studies. The UV cut off region (λ_{max}) lies around 200 nm and the crystal is absolutely transparent from 220–800 nm suggesting its application as NLO material. The thermal stability of the crystal was determined by thermogravimetric and differential thermal analyses. Laser damage threshold of BV was found to be 0.34 GW/cm^2 and hence BV can be used in frequency doubler system. Photoconductivity study of BV revealed negative photoconductiviting nature of the sample. The microhardness studies confirm that BV has a moderate Vickers hardness number (VHN) value in comparison to the other organic NLO crystals.

1 Introduction

A major effort was developed to use the nonlinear optical (NLO) effect in materials to generate frequencies that are not available and also to develop the capability of generating tunable coherent beams [1–4]. Much of this research has been directed towards materials that produce second harmonic generation (SHG), the frequency doubling of laser light, telecommunication, optical computing, optical data storage and optical information processing [5,6]. As a result, a variety of both organic and inorganic materials were grown [7–9]. Therefore materials with large second order optical nonlinearities, transparency at a wavelength involved and stable physicochemical properties are needed in order to realize many applications [10,11]. Considerable efforts have been made to combine amino acids with interesting organic acids, chlorides and inorganic materials to produce outstanding materials to challenge the existing NLO materials. As a result a number of amino acid based compounds are seen to impart NLO property in such organic crystals [12–15]. Recently Anand et al. has grown and characterized pure benzoyl glycine, and doped BG (benzophenone, iodine, copper and cadmium) single crystal using slow evaporation technique [16,17]. In this report we present our findings of our endeavour on the characterization studies like single crystal XRD, FTIR, H^1 and C^{13} NMR, TG/DTA, SHG, photoconductivity and microhardness studies so as to improvise this material for blue green laser radiation.

2 Synthesis

The starting materials benzoylchloride (E-Merck) and L-Valine (E-Merck) were commercially available. The required amount of L-Valine was dissolved in 10% of NaOH solution at a temperature of 30 °C. The appropriate amount of benzoyl chloride was added in successive stages to the solution. BV was formed in the form of precipitate. The precipitate was recrystallized thrice using acetone. The equation is

$$C_6H_5COCl + C_5H_{11}NO_2 \xrightarrow{10\%\ NaOH} C_{12}H_{15}NO_3 + HCl.$$

[a] e-mail: dpremanand@yahoo.co.in

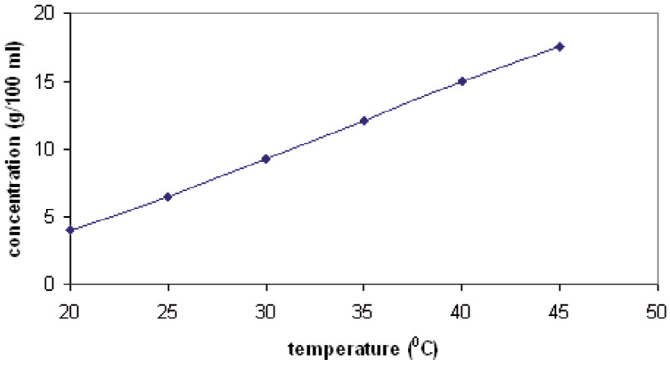

Fig. 1. Solubility curve of BV crystal.

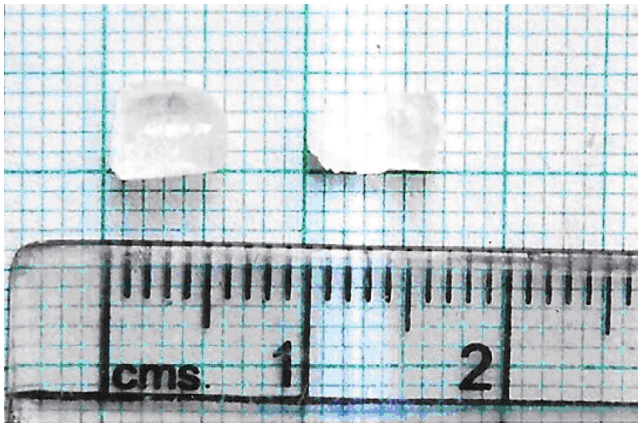

Fig. 2. (Color online) Single crystal of BV.

3 Solubility

The synthesized salt was used to measure the solubility of BV in acetone. A 250 ml glass beaker filled with 100 ml of acetone was placed inside a constant temperature bath whose temperature was set at 25 °C. An acrylic sheet with circular hole at the middle through which a spindle from an electric motor placed on the top of the sheet was introduced into the solution. A teflon paddle was attached at the end of the rod for stirring the solution. BV salt was added in small amount. The addition of salt and stirring were continued till the formation of precipitate, which confirmed the super saturation of the solution. Then, 20 ml of the saturated solution was pipeted out and poured into the petri dish of known weight. The solvent was completely evaporated by keeping the solution in open air for three days. The amount of salt present in 20 ml of the solution was measured by subtracting the weight of empty petri dish. From this, the amount of salt present in 100 ml of the solution was found out. In the same manner, the amount of the salt dissolved in 100 ml at 25, 30, 35, 40, 45 and 50 °C were found. Figure 1 shows the solubility curve of BV in acetone at different temperatures. It is seen from the solubility curve that the solubility of BV in acetone increases with increase in temperature. The solubility coefficient is an important parameter for studying the solubility diagram. Using the formula $(ds/dT)/S_0$, where S is the solubility (g/100 ml) and T is the temperature. S_0 is the solubility in g/100 ml corresponding to T_0, the temperature for which the solubility coefficient is determined [10]. Solubility coefficients per degree Celsius of T_0 values 25, 30, 35, 40 and 45 °C were calculated. The solubility coefficient is 0.03 per °C at 25, 30 and 35 °C and 0.04 per °C for temperatures studied. The regular behaviour in the solubility diagram makes BV suitable for the growth by temperature lowering and slow evaporation techniques using acetone as the solvent. The photograph of as grown crystals of BV was shown in Figure 2.

4 Single crystal XRD

The grown crystal was subjected to single crystal X-ray diffraction studies using an automatic diffractometer ENRAFNONIUS CAD 4 (The Netherlands) with MoK_α ($\lambda =$ 0.7170 Å) radiation and its unit cell dimensions are determined. The dimension of the crystal used for the measurement was $0.6 \times 0.4 \times 0.3$ mm^3. It is observed that the compound crystallizes in a non-centrosymmetric space group P21 of the monoclinic system with unit cell parameters $a = 5.49$ Å, $b = 5.12$ Å, $c = 21.894$ Å. The volume of the unit cell was found to be 611 Å^3.

5 FTIR studies

From the crystallographic data, it is inferred that L-Valine cation is in the Zwitterionic form. The FTIR spectrum of BV is shown in Figure 3. The amino group of L-Valine cation is protonated and the presence of NH_3^+ is confirmed through the existence of Zwitterionic nature of the molecule. The band at 3436 cm^{-1} in the infrared spectrum is attributed to the stretching vibration of N–H group. The absorption band at 3010 cm^{-1} is assigned to the aromatic C–H stretching vibration. The C=O stretching vibrations of COO^- is observed at 1688 cm^{-1}. Scissoring, twisting and wagging vibration of C–H of CH_2 in L-Valine molecules are observed at 1453, 1326 and 1026 cm^{-1}. The peak observed at 1446 cm^{-1} is assigned to the C–O asymmetric stretching vibration. The split band around 1600 cm^{-1} can be assigned to the bending vibration of N–H group [18]. The medium absorption band at 803 cm^{-1} corresponds to C–H out of plane bending vibration. The asymmetric and symmetric vibrations of the ionized carboxylate group are observed at 1602 cm^{-1} in infrared spectrum. Ratajczak et al. [19] reported that the absence of any strong IR band at 1700–1740 cm^{-1} corresponds to the vibrations of COO^- ion. This provides confirmation for the formation of the title crystal. Additionally the wagging type of vibration of NH_3 group is observed at 559 cm^{-1}. Thus the presence of functional groups was confirmed through FTIR analysis. Hence it can be concluded that the absence of C=O and NH_2 group frequencies and the presence of COO^- and NH_3^+ frequencies indicate that the molecule exists in zwitterionic form and the molecules are held by three dimension network of hydrogen bonds.

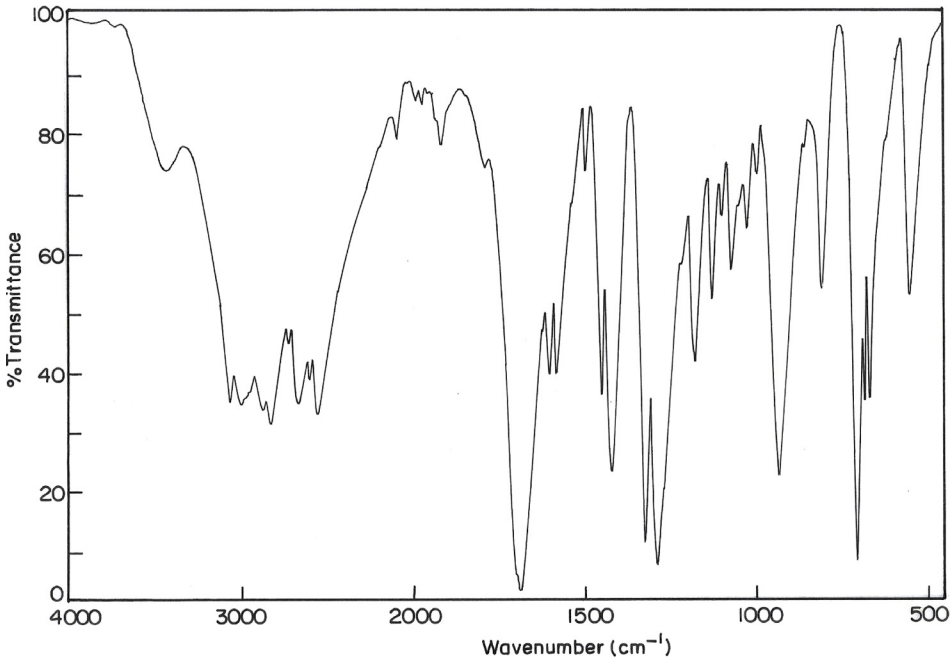

Fig. 3. FTIR spectrum of BV.

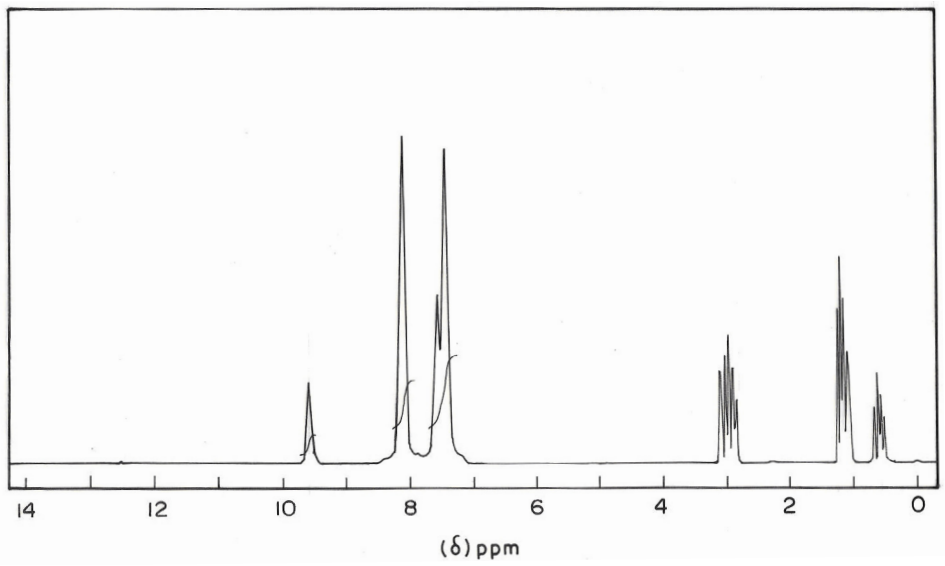

Fig. 4. H^1 NMR spectrum of BV.

6 ^{1}H and ^{13}C NMR

In order to determine the molecular structure, the hydrogen and carbon network in BV have been studied using these analyses. ^{1}H NMR and ^{13}C NMR spectrum of BV sample were recorded using JEOL: GSX 500 instrument in d^6-DMSO solvent with Tetramethylsilane (TMS) as an internal standard. Figures 4 and 5 represent ^{1}H and C^{13} NMR spectrum respectively. The ^{1}H NMR spectrum of the compound shows single proton multiplet at 0.80 ppm corresponding to single proton attached to $-C_2$- carbon. Similarly a single proton multiplet was also observed at 2.98 ppm due to proton present to the amide group. A sharp 6 proton multiplet was absorbed at 1.10 ppm corresponding gen-dimethly groups of valine moiety. A sharp singlet at 7.56 ppm can be attributed to 3 protons of the aromatic rings. Similarly a sharp singlet is also observed at 8.10 ppm can be attributed to presence of two proton preset at the ortho amide functional group. The peak at 9.40 ppm is due to the present of amide N–H group in the molecular structure. In the ^{13}C spectrum, the signal at 18.18 ppm represents the two methyl carbons. The peak at 31.25 ppm due to trustary carbon attached to two methyl groups. A peak at 58.32 ppm indicates a carbon attached nitrogen as well as carboxylic group. The signal at 168.91 indicates a carbonyl carbon attached to

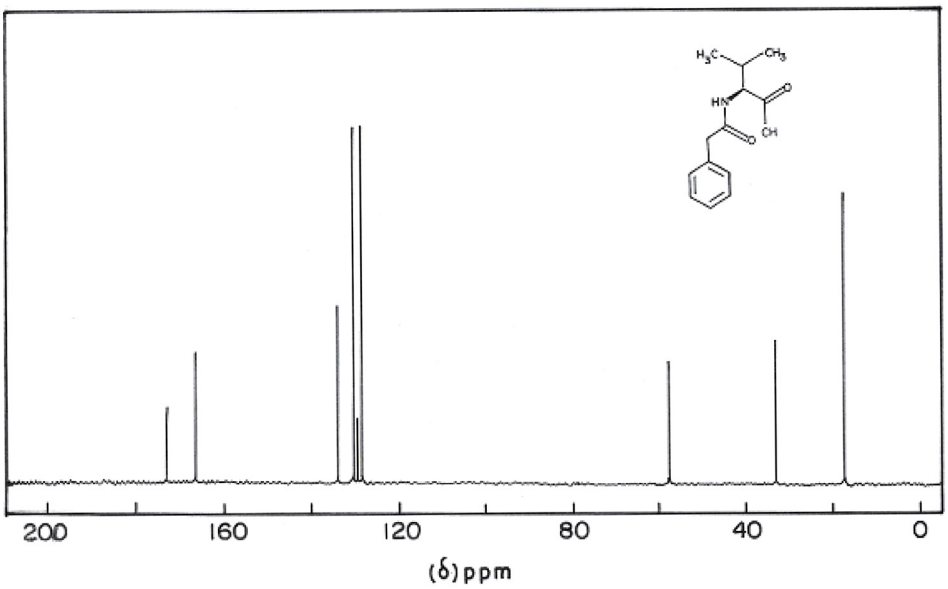

Fig. 5. C^{13} NMR spectrum of BV.

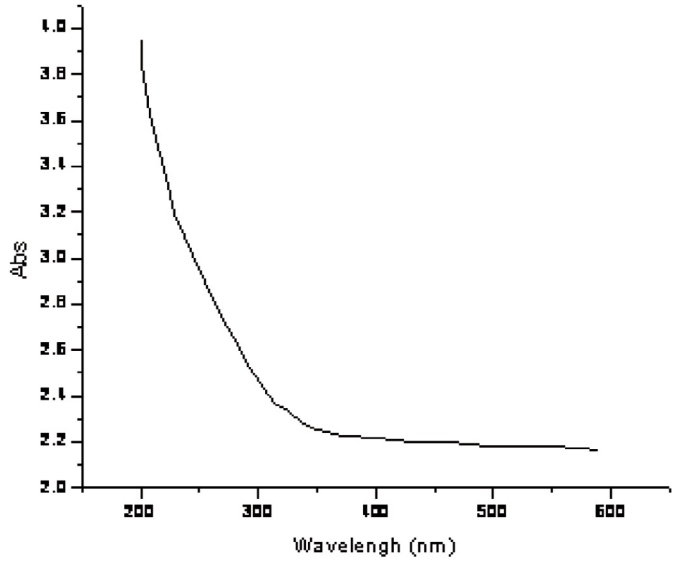

Fig. 6. Optical absorption spectrum of BV.

nitrogen and phenyl moiety. The peak at 174.39 ppm is representing the carboxylic acid carbonyl carbon.

7 Absorption spectrum

Optical transparency of the crystal was studied (Fig. 6) using Varian Carry 5E model Spectrophotometer. The UV-Vis-absorbance of the sample was scanned between 200 to 600 nm. The maximum wave length of the absorbance band was at recorded at 193 nm. The material is transparent in the range from 230 to 600 nm. The absence of absorption in the region between 230 to 600 nm indicates the non linear optical NLO behavior exhibited by such family of group of crystals. Thus it can be expended that BV is one of the potential candidate for use in optoelectronic devices.

8 Mass spectrum

Mass spectrum of BV sample was recorded (Fig. 7) using JEOL: GCmate instrument. In the mass spectrum shows appear of a molecular ions peak at m/z at 221, the base peak obtained at m/z 106 is due to the phenyl carbonyl radical ion.

9 TG/DTA

To analyze the thermal stability and confirm the melting point of the material, the thermogravametric (TG) and differential thermal analysis (DTA) were carried out in nitrogen atmosphere at a heating rate of 20 °C/min in the temperature range of 10 to 1200 °C using NETZSCH STA 409 C/CD. It is found from the TG trace that there is a weight loss observed and undergoes an irreversible endothermic transition at 195 °C. Figure 8 shows the TG/DTA curve of as grown crystal of BV.

10 Nonlinear optical properties

10.1 Powder SHG test

A quantitative measurement of the conversion efficiency of BV was estimated by Kurtz powder technique using a Q-switched Nd:YAG laser. A fundamental laser beam of 1064 nm wavelength, 8 ns pulse in depth with 10 Hz pulse rate was made to fall normally on the sample cell.

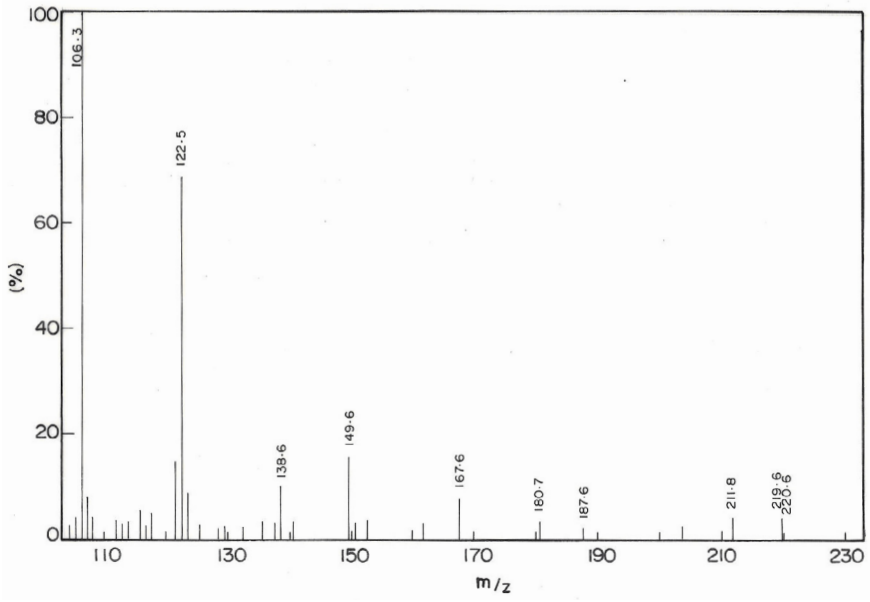

Fig. 7. Mass spectrum of BV.

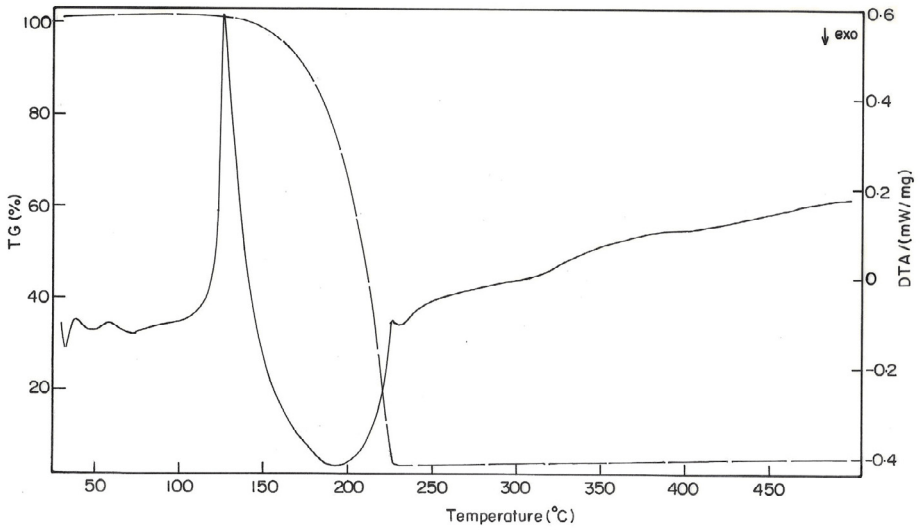

Fig. 8. TG/DTA of BV.

The power of the incident beam was measured using a power meter and it is 5.7 mJ/pulse. The crystal was grinded into powder and it was packed densely between two transparent glass slides. The emission of green radiation from the crystal confirmed the SHG in the crystal.

10.2 Second harmonic generation efficiency and phase matching cure

The fundamental wavelength emitted from a Q-switched Nd:YAG laser was used. A photodiode was used as a reference to monitor the pulse to pulse fluctuation in the input beam. BV sample was graded using standard sieves in the range less than 106 μm to above 150 μm. The measurement of SHG output for various particle size show the increasing SHG intensities with increasing particle size (Fig. 9) upto 150 μm, which confirm the phase matching behaviour of the material. Hence BV crystal can be used as an efficient frequency doubler and optical parametric oscillator provided if large-size single crystal are grown.

10.3 Laser damage threshold

Laser damage threshold of a material is defined as the maximum permissible optical power for a particular crystal to cause a breakdown of the material [20]. According to Nakatani et al. [21], the multiple shot (n-on-1) damage threshold is the minimum power level below which the crystal does not suffer damage after multiple shot pulses.

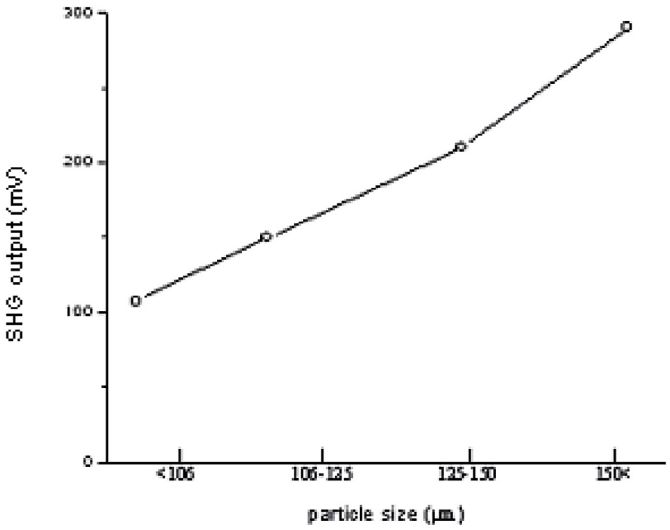

Fig. 9. Phase matching curve of BV.

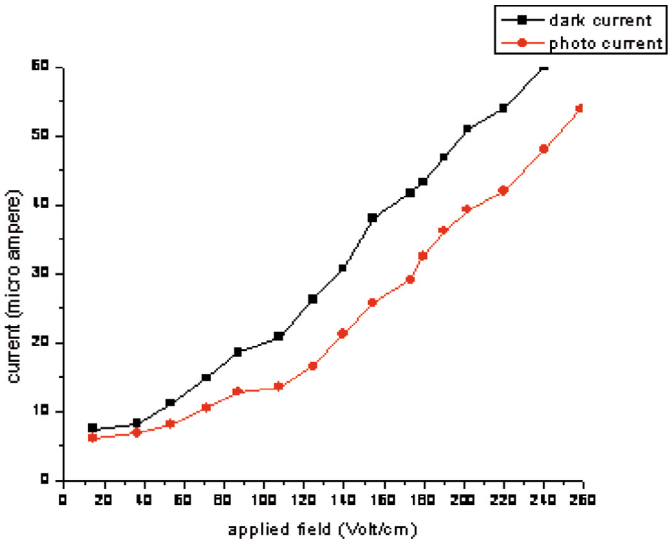

Fig. 10. (Color online) Field dependent conductivity of BV single crystal.

For crystals which are used in commercial frequency doublers, the multiple shot surface damage threshold is the most important parameter. In order to measure the laser damage threshold, as grown crystals of BV about 5 mm in diameter and 3 mm in thickness, were placed in front of a Q-switched Nd:YAG laser through slit (area 0.3 mm^2) following a focusing lens. Based on the multishot method, the damage was found visually. After that, the crystal was replaced by a power meter to measure the power density which was used to cause damage in the crystal. In the present work, laser damage was found to be 0.34 GW/cm^2 which is higher than that of KDP (0.2 GW/cm^2) as lower than that of urea (15 GW/cm^2). The high damage threshold reveals that the compound is chemically stable and neither hygroscopic nor soluble in water.

11 Photoconductivity studies

The photoconductivity studies of the BV single crystals were carried out using Keithley 480 picoammeter. In the absence of any radiation on the sample and by varying the applied field from 20 to 240 V/cm, the corresponding dark current values were recorded by the picoammeter. To measure the photo current the sample was illuminated with a halogen lamp (100 W) containing iodine vapour, by focusing a spot of light on the sample with the help of a convex lens. The applied voltage was increased from 20 to 240 V and the corresponding photo current was recorded. Photo current and dark current are plotted as a function of the applied field as shown in Figure 10. It is observed from the plot that the dark current is greater than the photo current, thus suggesting that BV exhibits negative photoconductivity.

The negative photo conductivity exhibited by the sample may be due to the reduction in number of charge carriers or their lifetime in the presence of radiation [22,23]. The decrease in lifetime with illumination could be due to the trapping process and increase in carrier velocity given by the relation

$$\tau = (vsN)^{-1}, \tag{1}$$

where v is the thermal velocity of the carriers, s in the capture cross-section of recombination centre and N is the carrier concentration. As intense light falls on the sample, the lifetimes decrease [24]. Stockman model explains the tendency of decrease in mobile charge carriers during negative photoconductivity. According to this model, for the BV crystal, the negative photoconductivity is based on the state between the Fermi level and the valence band [25]. This state has high-capture cross sections for electrons and holes. Also this state can capture electrons from the conduction band and holes from the valence band. Thus, the net number of mobile charge carriers is reduced due to incident radiation, giving rise to negative photoconductivity [26].

12 Microhardness studies

BV single crystal was subjected to Vickers microhardness test with the applied loads varying from 10 to 50 g for an indentation time of 10 s. Indentation was done on the well defined faces (110), (100) and (011) planes of the crystal. The Vickers microhardness values were calculated using the equation $H_v = 1.8544\ (P/d^2)\,kg/mm^2$. Vickers microhardness profile as a function of applied test loads is illustrated in Figure 11.

The value of the work hardening coefficient was estimated from the plot of $\log P$ versus $\log d$, drawn by the least square fit technique. It was observed that the Vickers hardness number increase with load. According to Onitsch, $1.0 \leq n \leq 1.6$ for hard materials and $n \geq 1.6$ for soft materials [27–29]. Hence, it is suggested that BV can be categorized as moderate materials.

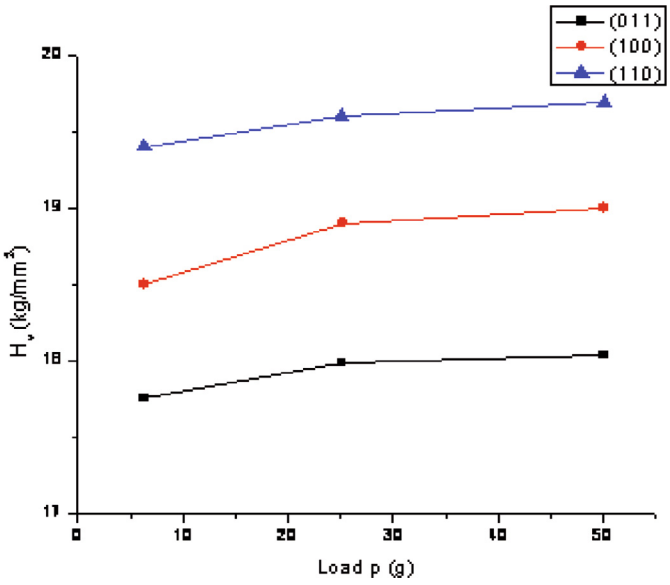

Fig. 11. (Color online) Variation on Vickers hardness number with applied load on (110), (100) and (011) plane.

13 Conclusions

BV was successfully grown by slow evaporation technique at room temperature. The cell parameter of the grown crystal was elucidated through single crystal XRD. The functional groups of BV crystalline sample were identified using FT-IR, ^{1}H and ^{13}C spectral analyses. Optical absorption spectrum confirms that the crystal exhibits nearly zero absorption in range 350–600 nm. Thermal analysis was carried out and the crystal is stable up to 195 °C. Owing to its SHG efficiency BV is considered as a promising material for NLO applications. Laser damage threshold of BV was found to be 0.34 GW/cm^2. Photoconductivity study of the material confirms the negative photoconductivity nature of the crystal. Microhardness studies indicate that the crystal has moderate VHN value.

It is a pleasure to acknowledge Dr. M. Vanjinathan, Lecturer, D.G. Vaishnav College, Chennai, India; Dr. Xavier, Department of Chemistry, Loyola College, Chennai and Dr. M. Palanichamy, Department of Chemistry, Anna University, Chennai for their constant help, support and encouragement.

References

1. M. Kitazawa, R.H. Higuchi, M. Takahashi, Appl. Phys. Lett. **64**, 2477 (1994)
2. L. Misoguti, A.T. Varela, F.D. Nunes, V.S. Bagnato, F.E.A. Melo, J. Mendes Filho, S.C. Zilio, Opt. Mater. **6**, 147 (1996)
3. W.S. Wang, M.D. Aggarwal, J. Choi, K. Bhat, T. Gebre, A.D. Shields, B.G. Penn, D.O. Frazier, J. Cryst. Growth **198**, 578 (1999)
4. W.T. Siltvast, *Laser fundamentals*, 2nd edn. (Cambridge University Press, 2004)
5. R.B. Lal, H.S. Zhang, W.S. Wang, M.D. Aggarwal, H.S.H. Lee, B.G. Benn, J. Cryst. Growth **174**, 393 (1997)
6. B.K. Periyasamy, R.S. Jebes, N. Gopalakrishnan, T. Balasubramaniam, Mater. Lett. **61**, 4246 (2007)
7. S.K. Lam, M.A. Chan, V. Lo, Opt. Mater. **18**, 235 (2001)
8. X. Wang, D. Xu, M. Lu, D. Yuvan, J. Huang, X. Cheng, S. Wang, S. Guo, G. Zhang, M. Pan, X. Duan, Z. Yang, Phys. Stat. Sol. A **191**, 106 (2002)
9. J. Zaccaro, J. Barruchel, A. Ibanez, J. Mater. Chem. **9**, 403 (1999)
10. V.A. Kuznetsov, T.M. Okhrimenko, M. Rak, Proc. SPIE **100**, 3178 (1997)
11. V.V. Kuznetso, T.M. Okhrimenko, M. Rak, J. Cryst. Growth **164**, 173 (1998)
12. M. Arivanandhan, A.R. Lakshi, R. Rathika, R. Gopalakrishnan, C.S. Raj, K. Shankaranarayan, Opt. Commun. **251**, 172 (2007)
13. B.K. Periyasmy, R.S. Jebas, N. Gopala Krishnan, T. Ba, M.N. Bhat, S.M. Dharma Prakash, J. Cryst. Growth **242**, 245 (2002)
14. A. Datta, S.K. Pati, J. Chem. Phys. **118**, 8420 (2003)
15. R. Ittyachan, P.C. Thomas, D.P. Anand, M. Palanichamy, P. Sagayaraj, Mater. Chem. Phys. **93**, 272 (2005)
16. T.K. Kumar, S. Janarthanan, S.M. Ravikumar, S. Pandi, M. Vimalan, P. Sagayaraj, D.P. Anand, J. Mater. Sci. Technol. **24**, 891 (2008)
17. D.P. Anand, S. Selvakumar, K. Ambujam, K. Rajarajan, M. Gulam Mohammed, P. Sagayaraj, Indian J. Pure Appl. Phys. **43**, 863 (2005)
18. L.T. Beuamy, *The infrared spectra of complex molecules* (J. Wiley & Sons, Inc., New York, 1954)
19. H. Ratajczak, J. Barycki, A. Pietraszko, J. Baran, S. Debrus, M. May, J. Venturini, J. Mol. Struct. **526**, 269 (2000)
20. S. Dhanuskodi, A.P. Jeyakumari, S. Manivannan, J. Philip, S.K. Tiwari, Spectrochim. Acta Part A **66**, 318 (2007)
21. H. Nakatani, W.R. Bosenberg, L.K. Cheng, C.L. Tang, Appl. Phys. Lett. **53**, 2587 (1978)
22. U.V. Hundelshausen, Phys. Lett. A **34**, 405 (1971)
23. R.H. Bube, *Photoconductivity of Solids* (Wiley, New York, 1981)
24. I.M. Ashraf, H.A. Elshaik, A.M. Badr, Cryst. Res. Technol. **39**, 63 (2004)
25. S. Pandi, D. Jayaraman, Mater. Chem. Phys. **71**, 314 (2001)
26. V.N. Joshi, *Photoconductivity* (Marcel Dekker, New York, 1990)
27. E.E.A. Shepherd, J.N. Sherwood, G.S. Simpson, J. Cryst. Growth **167**, 709 (1996)
28. R.I. Ristic, B.Y. Shekunov, J.N. Sherwood, J. Cryst. Growth **167**, 693 (1996)
29. R.T. Bailey, F.R. Cruicksharnk, D. Pugh, J.N. Sherwood, G.S. Simpson, S. Wilkie, J. Appl. Phys. **78**, 1388 (1995)